Biol Cybern (2010) 103:285–297
DOI 10.1007/s00422-010-0398-2

ORIGINAL PAPER

Biological Cybernetics

Compact internal representation of dynamic situations: neural network implementing the causality principle

José Antonio Villacorta-Atienza · Manuel G. Velarde · Valeri A. Makarov

Received: 17 December 2009 / Accepted: 16 June 2010 / Published online: 30 June 2010

Abstract Animals for survival in complex, time-evolving environments can estimate in a "single parallel run" the fitness of different alternatives. Understanding of how the brain makes an effective compact internal representation (CIR) of such dynamic situations is a challenging problem. We propose an artificial neural network capable of creating CIRs of dynamic situations describing the behavior of a mobile agent in an environment with moving obstacles. The network exploits in a mental world model the principle of causality, which enables reduction of the time-dependent structure of real situations to compact static patterns. It is achieved through two concurrent processes. First, a wavefront representing the agent's virtual present interacts with mobile and immobile obstacles forming static effective obstacles in the network space. The dynamics of the corresponding neurons in the virtual past is frozen. Then the diffusion-like process relaxes the remaining neurons to a stable steady state, i.e., a CIR is given by a single point in the multidimensional phase space. Such CIRs can be unfolded into real space for execution of motor actions, which allows a flexible task-dependent path planning in realistic time-evolving environments. Besides, the proposed network can also work as a part of "autonomous thinking", i.e., some mental situations can be supplied for evaluation without direct motor execution. Finally we hypothesize the existence of a specific neuronal population responsible for detection of possible time-space coincidences of the animal and moving obstacles.

J. A. Villacorta-Atienza · M. G. Velarde
Instituto Pluridisciplinar, Universidad Complutense,
Paseo Juan XXIII, 1, 28040 Madrid, Spain

V. A. Makarov (✉)
Departamento de Matemática Aplicada, Facultad de CC
Matemáticas, Universidad Complutense, Avda. Complutense s/n,
28040 Madrid, Spain
e-mail: vmakarov@mat.ucm.es

Keywords Internal representation · Neural networks · Situation models · Spatiotemporal dynamics

1 Introduction

The real world is a continuously changing environment whose complexity may compromise rigid reactive behaviors. Animals during long evolution developed mechanisms that enable predicting the future and a purpose-based selection of behaviors. Growing experimental evidence (for review see, e.g., Moser and Moser 2008; Savelli et al. 2008) suggests that these mechanisms rely on the ability of generating an Internal Representation (IR) of the body and external environment and on the parallel virtual "simulation" of multiple alternatives. In the context of an agent (either animal or robot) moving in an arena containing mobile and immobile obstacles, IR can be defined as an abstract, purpose-based spatiotemporal construction mimicking crucial features of the environment and describing the possible (including forthcoming) interactions between its elements and the agent. Thus IR should account both for spatial (static) structure of the environment and for time-dependent changes (moving obstacles).

Four main types of neurons involved in construction of the abstract IR of spatial environments have been reported. In their pioneering study O'Keefe and Dostrovsky (1971) proved the existence of a hippocampal neuronal population whose activity correlates with the animal's position in the environment. Moreover, they showed that this activity does not depend on the animal's orientation. When a rat moves in a known environment and reaches a specific spatial location the corresponding *place cell* increases its firing rate. The rate returns to the base line when the animal moves away from the place (O'Keefe and Dostrovsky 1971; Barry et al. 2006). The complementary information, also independent

of the animal's position, is provided by *head-direction cells* mainly found in the anterior thalamus, presubiculum, and lateral mammillary bodies (Taube et al. 1990a,b). These neurons respond according to the direction pointing by the animal's head. More recently a new type of neurons, so-called *grid cells*, has been discovered in the dorsocaudal medial entorhinal cortex, providing a structured IR of the surrounding space (Hafting et al. 2005; Moser et al. 2008). A grid cell fires at specific animal's locations given by vertexes of a triangular or hexagonal grid "covering" the environment. The orientation of the grid field may be controlled by the head-direction cells. It has also been shown that there exists a population of neurons in the entorhinal cortex responding to the presence of obstacles (i.e., object borders) (Savelli et al. 2008). The activity of the *border cells* is related to the orientation of obstacles and it correlates with the activity of grid and head-direction cells (Savelli et al. 2008; Solstad et al. 2008). This suggests that border cells contribute to the creation of a reference frame for grid and position cells.

The above mentioned studies provide experimental ground for the representation of surrounding space and static situations, however, dynamic (i.e., essentially time dependent) situations claim a spatiotemporal IR capable of dealing with time-changing environments (Sharma et al. 2003). Then IR must be based on two key elements: (i) *the world mental model* including both the agent and its environment; and (ii) *the principle of causality*.

The first component is widely accepted (see, e.g., Holland and Goodman 2003) and can be viewed as a description (not necessarily complete) of geometrical and physical laws governing the observed dynamical processes. For example, a free falling object accelerates with 9.81 ms^{-2} in the Earth. Experiments with astronauts catching a ball under reduced effective gravity revealed that the peak of anticipatory muscle activation occurs earlier than the real impact of the ball (McIntyre et al. 2001). After a few days the astronauts adapted to the new effective gravity conditions. This finding leads to two inferences: the brain has an internal mental model which "calculates" the ball trajectory and this model can be tuned by learning. Many other psychophysiological studies show that humans tend to represent observed and imagined (e.g., through reading) situations as dynamic structures and anticipate forthcoming changes.

The second IR component, the principle of causality, is implicit for every time-dependent process and it is strongly linked with the notion of the past and future. Any event in the present has a cause in the past and a consequence in the future, but not vice versa. In the IR context it means that the future is "open", i.e., it can be and should be predicted, but the past is "frozen" (unchangeable), i.e., obstacle's movements that happen in the space-time sense behind the agent cannot cause future collisions. As we shall show below this "static" nature of the past makes possible in mental simulations mapping of moving obstacles into time-invariant structures. This in turn offers a biologically plausible mechanism to compile dynamic situations into a *compact* internal representations (CIRs), suitable to be easily evaluated, stored, and recovered by the agent.

The existence of neuroanatomical substrates responsible for the high-level time-dependent functions mentioned above has been supported by the finding of *mirror neurons* (Rizzolatti et al. 2001). These cells even in anticipation respond both when a subject makes a particular action and when he sees how another individual performs the same action. However, more intriguing is that mirror neurons can react on the intention to perform a purpose-based action. When a monkey sees the initial phase of the action of extending a hand to grasp something (cause), specific neurons fire even if the final consequence, i.e., grasping (effect), is not directly perceived (Umiltá et al. 2001). Thus up-to-date neuroanatomical and electrophysiological studies converge to the hypothesis that the brain has specific spatially distributed neural networks (presumable in the hippocampus and neocortex) responsible for IR of static as well as dynamic situations, which may offer multiple, in fact countless, ways of performing behaviors.

Recent theoretical research on IR (although the first record goes back to 1943, Craik 1943) elucidated its main advantage: it allows detaching the behavior from direct environmental control by, e.g., inhibition of the motor execution (Hesslow 2002; Cruse 2003; Kuhn and Cruse 2005; Aitkenhead and McDonald 2006; Mohan and Morasso 2007). This enables responses of the organism to features of the world that are not directly present and hence to appropriately plan ahead. Besides, IR can be evoked mentally (without direct sensory input) to evaluate potential solutions. It is widely believed that IR is a prerequisite of a cognitive behavior (Cruse 2003). Particularly, the IR concept has been used to control a multisegmented manipulator with redundant degrees of freedom (Steinkuhler and Cruse 1998). Specific feed-forward networks and Recurrent Neural Networks (RNNs) have been used as holistic models of geometrical structures like bodies with arms and legs (see, e.g., Mohan and Morasso 2007; Kühn et al. 2007 and references therein). It has been shown that such networks can operate as forward models, inverse models or any mixed combination. Later in a series of articles (Kühn et al. 2007; Kühn and Cruse 2007; Cruse and Hübner 2008; Makarov et al. 2008) it has been argued that IR based on RNNs assembled using simple building blocks can implement working memory. Namely, it has been shown that RNNs can store and then reproduce some specific static and dynamic situations. We have shown that a network of n neurons can learn and then replicate a sequence of up to n different frames (Makarov et al. 2008). Another promising application of the IR approach is the construction of sensory-motor maps that implement external anticipation of

the sensory information. For example, it has been shown that echo state networks can successively learn forward models for a blind navigation in a square shaped static environment (Svensson et al. 2009). Toussaint (2006) argued that standard sensory-motor maps lack a proper neural representation and proposed the use of neural field models. Then motor activations induce anticipatory shifts of the activity peak in the sensory-motor map, which in turn can be used more naturally for planning and navigation in a maze.

In the present study we propose an Internal Representation Neural Network (IRNN) capable of dealing with dynamic situations, i.e., when a mobile agent has to cope with an environment also containing moving objects (obstacles). In such a situation the quasistatic approach or sequential behaviors, as proposed by Kuhn and Cruse (2005) for language production, may not work properly. Instead we formulate the model and study its behaviors in the framework of the dynamical systems theory. Thus the mental simulations of behaviors occur through operations feasible in the phase space of the IRNN and their results also belong to this space. Hence an IR (as a result of simulation) is an element of the phase space whose desired properties are: (a) mental calculations should converge to the same (or similar) IR under small perturbations and (b) IR should admit a compact description ready to be stored in (static) memory and allowing operations like classification, grouping, averaging, etc. We show that the IRNN satisfies both properties and the generated CIRs of dynamic situations can be associated with the simplest form of attractors, i.e., stable steady states. Thus time-evolving situations are represented by time-invariant objects. Finally, the strategies or, more particularly, admissible trajectories for the agent are defined by the position of the steady state in the multidimensional phase space, i.e., the CIRs can be unfolded into the real space.

2 General architecture of IRNN

Let us consider an agent moving in a time-dependent environment with the objective to reach a target (Fig. 1a). For the sake of simplicity (but see Sect. 6) the target is considered immobile and can be an object or a specific place or even an area in the arena. We assume that the target emits or reflects a sensory signal, e.g., sound or light, which is perceived by the agent (i.e., the target is "visible", although its perceiving may not be 100% robust). In general, we assume that a path to the target can be found, e.g., by employing a searching algorithm like chemotaxis or infotaxis (Berg and Purcell 1977; Berg 1993; Vergassola et al. 2007). However, in our case the agent has an additional difficulty: the presence of moving (besides immobile) obstacles in the arena, which should be avoided. All obstacles are also "visible", hence the agent can make a non-blind decision. This is attained by constructing

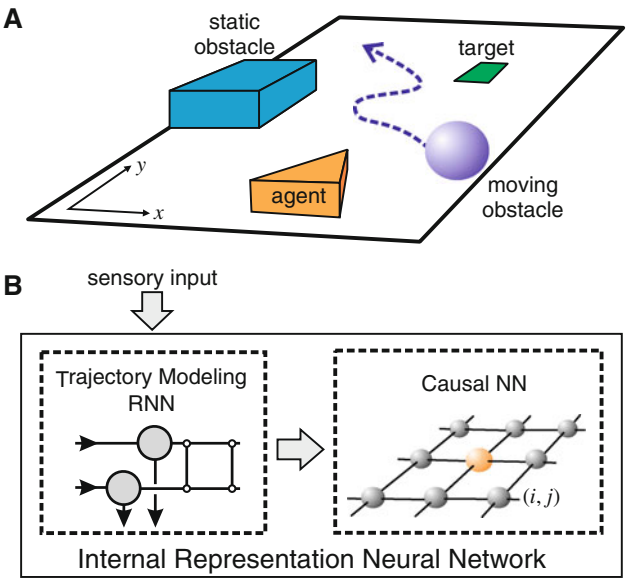

Fig. 1 **a** Sketch of an arena containing agent, target, and static and moving obstacles. The agent perceives all objects in the arena and creates an internal spatiotemporal representation of itself and of the environment with the goal of reaching the target avoiding collisions with the obstacles. **b** General block-scheme architecture of the IRNN consisting of two coupled subnetworks: (i) Trajectory Modeling and (ii) Causal neural networks. The TM-RNN receives sensory information, simulates trajectories of all objects (except the agent) and maps them into the CNN, which creates the CIR of the dynamic situation

a spatiotemporal IR of the dynamic situation, i.e., of a conjunction of the environment and the agent features significant for achieving the goal. To perform this task the agent besides mapping the stationary structure of the arena into an abstract IR should also be capable of making prediction on the possible positions of the obstacles and itself in the (mental) future and resolve collisions.

Figure 1b shows the general architecture of the agent's IRNN. It consists of two coupled subnetworks: Trajectory Modeling RNN (TM-RNN) and Causal Neural Network (CNN). The TM-RNN receives a sensory information either directly from the sensory system or from another brain area (e.g., memory). In the latter case the IRNN takes part in completely or partially mental (i.e., without direct observation of the environment) simulations of dynamic situations. The TM-RNN should be trained by real trajectories. Once the training is deemed finished the network becomes capable of simulating arbitrary trajectories of objects using as an input only their initial conditions (e.g., position and velocity) in a similar way as it has been observed in experiments with astronauts under reduced gravity (McIntyre et al. 2001).

To create a suitable IR the agent has to synchronize its possible motions with those given by the TM-RNN for the obstacles. This is achieved in the CNN that is a two dimensional ($N \times M$) lattice of locally coupled neurons that geometrically reproduces the arena, i.e., position of a neuron in the lattice described by the pair of indexes (i, j) corresponds

to the actual (x, y)-coordinates in the arena (Fig. 1). Such mapping is the simplest but not unique. For example, to gain better realism the mapping may be logarithmic, i.e., the distance in the real space scales logarithmically into the neuronal lattice (see, e.g., Hafting et al. 2005 for grid cells). The assumption that the agent possesses all necessary information on the environment (all objects are "visible") suggests the egocentric reference frame for the CNN, i.e., the agent maps itself into the origin of the neuronal lattice (red bigger neuron in Fig. 1b). Such reference frame has been argued to be used by insects (Collett and Zeil 1998), although more complex navigational systems have hierarchical organization depending on the context. For instance, honeybees switch between the egocentric and allocentric reference frames depending on whether they are flying along an unknown or a familiar route, respectively (Menzel et al. 2000).

3 Compact internal representation of complex environments

IR is a task-oriented reflection of the environment and the agent, which offers distinct modes to fulfill the task. For illustration in what follows we chose one specific decision making problem: a search for paths to the target (e.g., the shortest or safest, i.e., one can minimize, e.g., the risk of crashing against an obstacle or/and the length of the path.).

Emergence of a CIR in the IRNN can be viewed as a result of *virtual exploration* of the environment. Conceptually, a number of identical virtual agents start from the agent's initial position and perform a random search in the lattice space until they explore completely the "arena" or some of them reach the target image in the CNN. Then the distribution of the virtual agents in the CNN lattice defines the CIR and the optimal strategy.

3.1 Static environments

Let us first describe how CIR can be created in the simplest case when all elements in a 2D arena (except the agent) are immobile. Then the output of the TM-RNN (Fig. 1b) is time independent, and hence it just maps the immobile objects into the CNN whose dynamics models the process of virtual exploration

$$\dot{r}_{ij} = d\,\Delta r_{ij} - r_{ij}\,p_{ij} \tag{1}$$

where r_{ij} is the neuron state variable, representing the concentration of virtual agents at the cell (i, j); the time derivative is taken with respect to the *mental* (inner) time τ; $\Delta r_{ij} = r_{i+1,j} + r_{i-1,j} + r_{i,j+1} + r_{i,j-1} - 4r_{ij}$ denotes the discrete Laplace operator describing the local (nearest neighbor) interneuronal coupling, whose strength is controlled by d; and p_{ij} accounts for the target:

$$p_{ij} = \begin{cases} 1, & \text{if } (i, j) \text{ is occupied by target} \\ 0, & \text{otherwise} \end{cases} \tag{2}$$

It is worth pointing out that a target is not a real entity (as an object or place) existing in the environment, instead it is designated by the agent's motivation layer. For example, a football player can turn aside from or catch a ball depending on which side he plays on. Thus the target is not an external constraint but an internal emergent property of the brain, whose influence we model by the reactive term in (1). This differs from other approaches that postulate targets as singular elements in the environment (see, e.g., Schmidt and Azarm 1992). In contrast, here obstacles are indeed external constraints whose biological identity, provided by boundary cells (Savelli et al. 2008), suggests that they shape the IR through altering states of the neurons corresponding to the obstacle boundaries. We assume that the obstacles are solid non-penetrable objects, hence a virtual agent reaching an obstacle frontier rebounds and continues exploring the arena. Thus we impose zero-flux (Neumann) boundary conditions at the obstacle's frontiers and also at the arena boundary.

Stable steady states are the only attractors in the phase space $\Psi = \mathbb{R}_+^{NM}$ of the dynamical system (1) (Appendix 7). At $\tau = 0$ no virtual agent exists, hence we set $r_{ij}(0) = 0$ for all CNN cells except those occupied by the agent, where $r_{ij}(\tau) = r_a$ for $\tau \geq 0$. Then the trajectory in Ψ defined by these initial conditions tends to one of the steady states $r^*_{ij} \in \Psi$, which is the CIR of the given static situation. By unfolding this steady state into the three-dimensional lattice space $\{\mathbb{Z}^2, \mathbb{R}_+\}$ we get a stationary pattern that can be used to trace curves or paths starting at the agent location and crossing normally the contour lines. We note that r^*_{ij} satisfies the Laplace equation, and consequently the created pattern has no local minimums (Louste and Liegeois 2000; Keymeulen and Decuyper 1994). This ensures that all paths (except a null set) derived from this approach end at the target, and hence we obtain multiple alternatives to reach the target.

The described dynamical process yielding the CIR has certain similarities with the classical diffusion in a 2D reservoir used by Schmidt and Azarm (1992) for the path planning. However, in the classical approach: (i) the agent is not explicitly present in the model, while the target is postulated; and (ii) the obstacles absorb the diffusing substance (zero boundary conditions). To illustrate the differences we performed two simulations involving the classical and IRNN approaches.

Figure 2a shows an example of the potential field and paths to the target obtained using the classical diffusion with zero boundary conditions at the obstacle and arena frontiers. The target is a source of a "gas" that freely diffuses forming a potential field. Then valid paths are curves radially leaving the target position and perpendicular to the contour lines. As

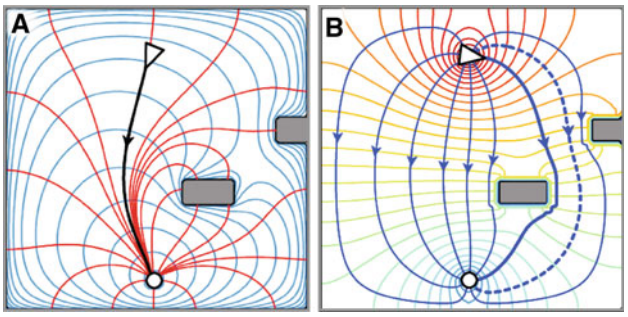

Fig. 2 Moving in a static environment. **a** Classic 2D diffusion with a constant source at the target position (marked by *circle*) creates potential field with a single maximum and several saddle points. Then there exists a *unique* path from the agent (*triangle*) avoiding obstacles (*grey rectangles*) to the target. **b** The IRNN approach yields a set of paths starting at the agent position and ending at the target. The agent is free to chose among different alternatives, e.g., by minimizing the path length (*solid thick curve*) or by rising safety (*dashed curve*), under additional constraint that it must pass between the two obstacles. Parameter values: (60×60) lattice, $r_a = 1$, $d = 2.5$, and the integration time $\tau_{end} = 10^3$

a consequence there exists a unique trajectory connecting the target and location where the agent is supposed to be (Fig. 2a, thick line).

Figure 2b shows the pattern r^*_{ij} (concentration of virtual agents) obtained by the IRNN. We notice that the explicit modeling of the agent leads to multiple curves connecting the agent and the target locations. Thus we achieve a CIR, where the agent has freedom to chose among different alternatives. We also notice that the pattern (Fig. 2b) has smooth transitions between actual obstacles and empty space. This accounts for uncertainty in the obstacle dimensions and positions. Then path planning from the agent to the target can naturally include the level of safety, e.g., a cost function that describes the risk of collision against the length of the path. The strategy can also include additional conditions, such as to pass through the gap between two obstacles (dashed curve vs. thick solid curve in Fig. 2b), which is impossible in the classical approach.

3.2 Dynamic environments

The above discussed IR of static environments cannot be applied directly to dynamic situations. However, we shall show now how the moving obstacles can be mapped into static images in the CNN lattice space, and hence the problem can be reduced to the *effectively* static case.

To illustrate the concept let us consider an arena with a single moving obstacle (Fig. 3a). For simplicity we assume that the agent velocity $|v_{ag}|$ is constant. Then at $\tau = 0$ a set of virtual agents is released into the CNN at the agent initial position. These agents start exploring the environment, which yields a wavefront composed of those virtual agents that reached the points furthest away from the agent initial position. The wavefront can be viewed as the "present" in the mental time τ, dividing the three dimensional spacetime (2D space + time) into two disjoint sets corresponding to the points in the (mental) past and in the future. The part of the CNN that has been visited by a virtual agent will be related to the virtual past, while the rest is in the future (Fig. 3b). Thus all neurons inside the area enclosed by the wavefront belong to the virtual past and those outside the area belong to the virtual future.

Due to the principle of causality none of the events occurring ahead of the wavefront (in the virtual future) can affect those behind it (in the virtual past). This allows restricting the predicted motion of the obstacle (and hence collisions possible in the virtual future) to the lattice space outward the wavefront (Fig. 3b, gray vs. blue obstacle parts). As the mental time τ proceeds, a circular wavefront formed by the furthest virtual agents expands until the obstacle will be reached. The spatial locations where the wavefront coincides with the obstacle (Fig. 3b, yellow circle) correspond to agent-obstacle

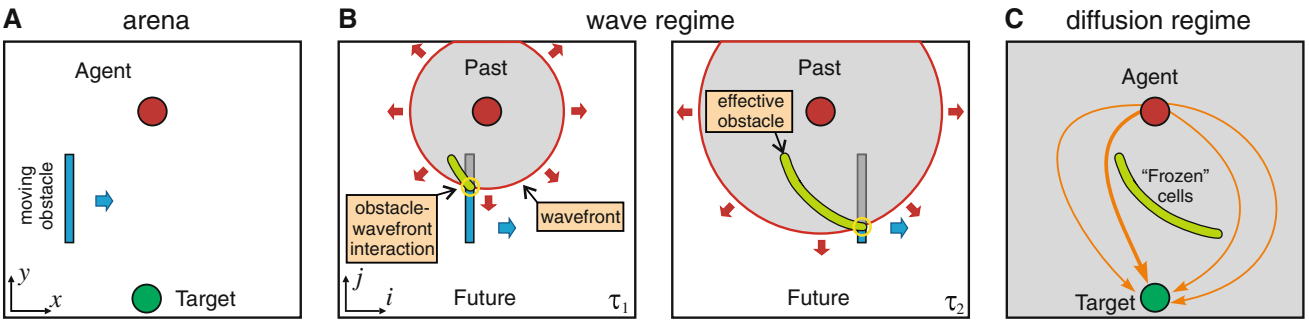

Fig. 3 CIR of a dynamic situation. **a** 2D arena consists of an agent (*red circle*), a target (*green circle*), and a moving obstacle (*blue rectangle*). **b** Three dimensional spacetime plots sketching the wave regime in the CNN. The expanding wavefront separates the agent virtual past from the future (*grey* and *white* areas, respectively). Effective influence of the moving obstacle over the agent is restricted to the isochronous spatiotemporal points of the wavefront and moving obstacle (*yellow circle*). This encloses a set of frozen neurons (*green area*), which form the effective obstacle. **c** The diffusion regime (behind the wavefront) as in Fig. 2b shapes the CIR of the dynamic situation and enables the decision making

collisions in the virtual present that should be avoided at the motor execution. With the time course these spatial locations (forbidden to be visited by the agent) delimit a set of neurons (Fig. 3b, green area), which progressively leads to formation of a static *effective* obstacle. Since these neurons belong to the virtual past, new events cannot change their state, hence their dynamics can be "frozen". Thus the principle of causality in the IR context converts moving obstacles into time-independent effective obstacles, i.e., makes the past effectively static.

Once the effective obstacle has been formed and the wavefront has passed, the IR problem reduces to the previous static case. Hence we can apply the approach illustrated in Fig. 2b. Then the steady state pattern r_{ij}^* obtained for the new effectively static situation gives the CIR of the dynamic situation and ensures that all feasible paths will avoid the moving obstacle (Fig. 3c). Thus the CIR of the dynamic situations is obtained in two steps:

1. Wave regime. Propagation of the wavefront separating the virtual future from the virtual past. Effective obstacles are formed in the CNN.
2. Diffusion regime. Evolution of the CNN with effective (immobile) obstacles shapes the CIR.

Notice that both regimes occur simultaneously in the virtual mental time, but belong to different spatial regions in the CNN lattice.

4 IRNN implementation

The IRNN consists of two interacting subnetworks (Fig. 1b). In this section we provide their formal neuronal implementation.

4.1 Trajectory modeling neural network

An accurate prediction of trajectories of moving objects results from previous learning (McIntyre et al. 2001), i.e., observation of moving objects tunes the neural network designed for the prediction. Recently we have discussed elements for a general memory structure (Makarov et al. 2008), and proposed an RNN capable of learning and replicating some specific dynamic situations. The trajectory of a moving object can also be viewed as an example of such a dynamic situation. Thus the general RNN-based concept can be applied to the learning and modeling trajectories of moving objects.

Let $F(t) = (x(t), y(t))$ be a 2D-trajectory of an object that passes at $t = 0$ through a point (x_0, y_0). Then the prediction or modeling of the object trajectory consists in estimating a function $\hat{F}(\tau) = (\hat{x}(\tau), \hat{y}(\tau))$ that approximates $F(t)$ for $t \geq 0$ based on the observation of the past (i.e., $\hat{F}(t) \approx F(t)$ for $t \geq 0$). We note that the trajectory modeling actually is made by the TM-RNN in the mental time τ. Besides, the obtained trajectory represents the dynamics of, e.g., the geometrical center of the object, while the rest can be obtained by translation.

Developing $F(t)$ into a Taylor series we have

$$F(t) = F(0) + F'(0)t + \frac{F''(0)}{2}t^2 + \cdots \tag{3}$$

where $F(0) = (x_0, y_0)$, $F'(0) = (v_0, u_0)$, and $F''(0) = (a_0, b_0)$ are the object position, velocity, and acceleration at $t = 0$, respectively. The time derivatives are estimated (by the sensory system) from the object past ($t \leq 0$). We note that in the r.h.s. of (3) one can keep an arbitrary number of high order terms. However, their estimates require additional computational load and may not be reliable, since the error increases with the order. Thus for the x-component (similar for y) we have

$$\hat{x}(\tau) = x_0 + v_0\tau + \frac{a_0}{2}\tau^2, \quad \tau \geq 0 \tag{4}$$

Equation 4 has three parameters x_0, v_0, and a_0 defining the dynamic situation and thus requires a three-neuron RNN for the modeling. We assume that the agent has an inner time scale h that may vary between "species" and/or "individuals". This reduces the problem to discrete time $\tau = kh$. Figure 4a shows the TM-RNN composed of three Input Compensation (IC) units, whose internal discrete dynamics is given by (Kühn et al. 2007; Kühn and Cruse 2007; Makarov et al. 2008)

$$\zeta_j(k+1) = \begin{cases} \xi_j(k), & \text{if } \xi_j(k) \neq 0 \\ s_j(k), & \text{otherwise} \end{cases} \qquad 1 \leq j \leq 3 \tag{5}$$

where $s_j(k) = \sum_{i=1}^{3} w_{ji}\zeta_{ij}(k)$ is the internal recurrent input and $W = \{w_{ji}\}$ is the coupling matrix.

The TM-RNN can stay either in learning or in operational regime. In the operational regime the coupling matrix W is fixed and the network can replicate previously learned stimulus or model new trajectories. During learning the network is exposed to training stimuli. By a training stimulus we understand a sequence of 3D vectors $\xi(k) = (x(k), v(k), a(k))^T$, which represents a piece of an observed trajectory. Here

$$v(k) = \frac{x(k) - x(k-1)}{h}, \quad a(k) = \frac{v(k) - v(k-1)}{h} \tag{6}$$

are estimates of the velocity and acceleration obtained from the object observation. Training consists in appropriate adjustment of the coupling matrix W by using a learning rule, that can be described as teacher forcing based on the classical delta rule (Makarov et al. 2008)

$$W(k+1) = W(k)\left(I - \varepsilon\xi(k-1)\xi^T(k-1)\right) + \varepsilon\xi(k)\xi^T(k-1) \tag{7}$$

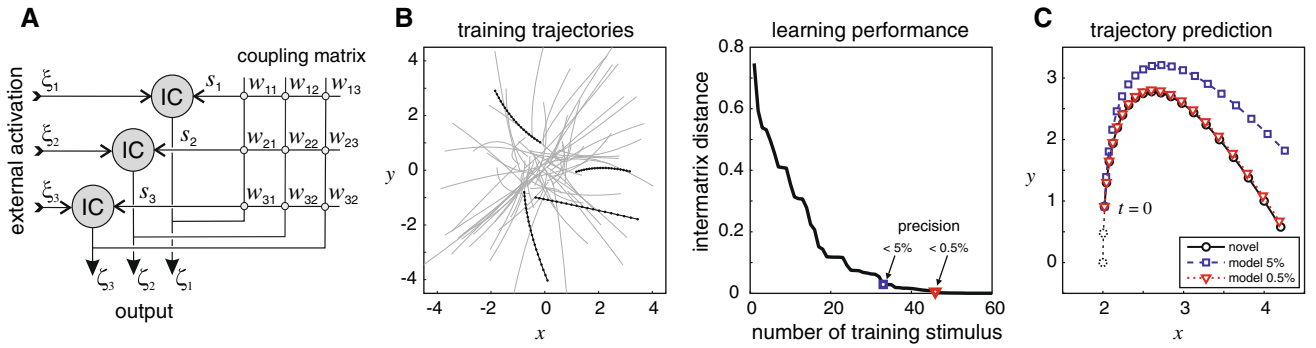

Fig. 4 Trajectory Modeling Recurrent Neural Network. **a** Circuit implementation of the TM-RNN. Three input compensation units are recurrently coupled through the matrix $W = \{w_{ij}\}$. External activation can be used either for learning (adjusting W) by presenting known trajectories of moving objects or for modeling by supplying initial conditions and reading out the network output. **b** Training TM-RNN. *Left panel*: trajectories used for learning (four arbitrary shown in black). *Right panel*: Convergence of the learning process. Intermatrix distance (8) is plotted versus the number of training trajectories presented during the learning ($h = 0.1$, $\varepsilon = 0.1$). **c** Trajectory modeling using coupling matrix W trained up to 5% (*squares*) and 0.5% (*triangles*) precision. *Circles* corresponds to the real trajectory. The first two points were used for evaluation of the initial object velocity and acceleration

where $\varepsilon > 0$ is the learning rate. To quantify the learning performance we use the normalized inter-matrix distance

$$d(k) = \frac{\|W(k) - W_\infty\|}{\|W_\infty\|} \tag{8}$$

where $W_\infty = \lim_{k\to\infty} W(k)$ is the limit (learned) matrix.

A thorough mathematical study of the RNN dynamics and the learning process is given in Makarov et al. (2008). Particularly, for $W(0) = 0$ Theorem 7, applied in our case, states that

$$W_\infty = (\xi(2), \xi(3), \xi(4))\,(\xi(1), \xi(2), \xi(3))^{-1} \tag{9}$$

which yields

$$W_\infty = \begin{pmatrix} 1 & h & h^2 \\ 0 & 1 & h \\ 0 & 0 & 1 \end{pmatrix} \tag{10}$$

We note that the limit coupling matrix does not depend on the external world parameters (e.g., particular trajectories, velocities, etc.) but only includes the inner time constant h. This means that the TM-RNN is universal and can be used for prediction of any type of movement. In fact, its generalization for prediction of more complex trajectories (retaining higher order terms in (3)) is straightforward.

To crosscheck the theoretical predictions and illustrate the trajectory learning and modeling properties of the TM-RNN we simulated 60 trajectories ($t_{\max} = 2$) with randomly chosen parameters, i.e., acceleration, initial velocity and position (Fig. 4b, left panel). The trajectories have been discretized ($h = 0.1$) and submitted to the network for training. Figure 4b (right panel) shows the learning performance, i.e., the time evolution of the intermatrix distance (8) between $W(k)$ and the theoretically predicted matrix (10). During the training $W(k)$ converges to W_∞ and the error decreases below 5% and 0.5% in about 35 and 45 stimulus presentations, respectively.

Once the learning was deemed finished (with a given precision) we tested the trajectory modeling capacity of the TM-RNN. We generated a novel trajectory (Fig. 4c, open circles curve), which has not been used for learning. The first three points of the trajectory have been used to estimate the initial vector $\xi(0)$ (i.e., the trajectory prediction requires an observation of its initial part). Then this vector has been submitted to the TM-RNN as external activation to simulate trajectories using the coupling matrices obtained at 5 and 0.5% precision (open squares and triangles in Fig. 4c, respectively). With 5% error the trajectory simulated by the network significantly diverges from the real one. However, with improved learning (10 additional training cycles) the simulated trajectory reproduces the real one with quite a high precision.

4.2 Causal neural network

The complete CNN is based on the lattice described in Sect. 3.1, but now each unit is a modified FitzHugh-Nagumo neuron, which yields the following dynamical system

$$\begin{aligned} \dot r_{ij} &= q_{ij}\left(H(r_{ij})\left[f(r_{ij}) - v_{ij}\right] + d\Delta r_{ij} - r_{ij}\,p_{ij}\right) \\ \dot v_{ij} &= (r_{ij} - 7v_{ij} - 2)/25 \end{aligned} \tag{11}$$

where v_{ij} is the so-called recovery variable; $f(r)$ is a cubic nonlinearity, which for numerical simulations we set to $f(r) = (-r^3 + 4r^2 - 2r - 2)/7$; and H is the regime controlling (Heaviside step) function:

$$H(r) = \begin{cases} 1, & \text{if } r \le r_{\rm h} \\ 0, & \text{otherwise} \end{cases}$$

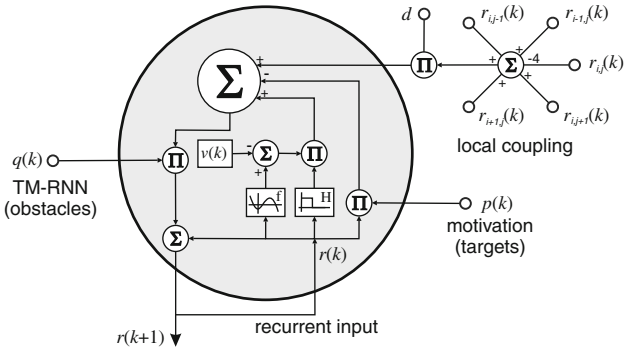

Fig. 5 Circuit implementation of the modified FitzHugh-Nagumo neuronal unit used in the CNN lattice (11). The blocks f, H, Σ, and Π stand for cubic nonlinearity, Heaviside step function, sum, and product, respectively. The block $v(k)$ updates the state of the corresponding recovery variable (linear sum of $r(k)$ and $v(k)$)

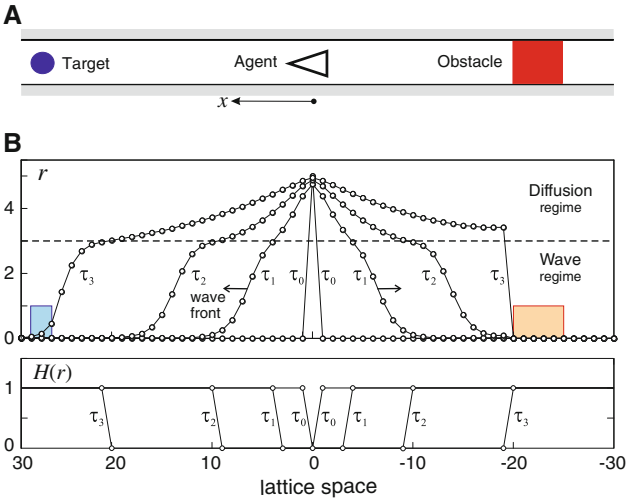

Fig. 6 Two-regime dynamics of the CNN in a 1D geometry. **a** One dimensional tunnel with an agent at $x = 0$. Target (*circle*) is in the left end of the tunnel, while the right end is closed by an obstacle (*square*). **b** Snapshots illustrating the evolution of the neuron states r_j (*top inset*) and of the regime controlling function $H(r)$ (*bottom inset*). A wavefront propagates below the dashed horizontal lines (Wave regime), meanwhile a passive diffusion happens above the line (Diffusion regime). Parameter values: $d = 0.2$, $r_a = 5$, and $r_h = 3$

where r_h is the threshold separating the wave and diffusion regimes.

The binary variable $q_{ij}(\tau) \in \{0, 1\}$ in (11) describes the influence of effective obstacles (green area in Fig. 3b) on the CNN dynamics. This inhibitory term mimicks the possible effect that border cells may exert over the activity of grid cells (Savelli et al. 2008). The TM-RNN provides the obstacle position, thus causing firing of the corresponding artificial border cell, which in turn inhibits the response of the CNN ("grid") cell r_{ij}. When the "border" cell is silent (no effective obstacle) r_{ij} evolves according to the CNN intrinsic dynamics.

At $\tau = 0$ no effective obstacle exists and $q_{ij}(0) = 1$ $\forall(i, j)$. For $\tau > 0$ a concentric circular wave (sketched in Fig. 3b) is generated. Once the wavefront catches up an obstacle (mobile or immobile) it slips around. Cells, where the wavefront "touches" an obstacle at $\tau = \tau_0$ (Fig. 3b, yellow circle) become "frozen", $q_{ij}(\tau \geq \tau_0) = 0$. As a consequence, for the frozen cells we have

$$r_{ij}(\tau) = r_{ij}(\tau_0), \quad \text{for } \tau \geq \tau_0 \tag{12}$$

Figure 5 shows the circuit implementation of the CNN unit operating in the discrete time k. The unit, besides its own recurrent feedback $r_{ij}(k)$, receives three types of inputs: (i) local coupling from the nearest neighbors, (ii) inhibitory signal modeling the presence of effective obstacles $q_{ij}(k)$ (provided by the TM-RNN), and (iii) motivational input defining target locations $p_{ij}(k)$ (given by (2)). The updated state $r_{ij}(k + 1)$ is readout at the unit output.

It can be shown that the unit's intrinsic dynamics (for $d = 0$, $p = 0$, $q = 1$, and $H = 1$) is bistable, with two stable steady states at $r_d = 0$ and $r_u = 3$. This yields multi-stability and even spatial chaos for a low enough coupling strength $d < d_{cr}$ (Nekorkin and Makarov 1995; Sepulchre and MacKay 1997; Nekorkin et al. 1997; Nekorkin and Velarde 2002). The upstate r_u has much bigger basin of attraction than the downstate r_d. For a strong coupling $d > d_{cr}$ by fixing just a single neuron in the upstate we create a wave that propagates with a constant velocity and switch all neurons from the downstate to the upstate. Hence to obtain a wavefront in our problem we select a high enough inter-neuronal coupling $d > d_{cr}$.

The propagating wave switches neurons to the upstate and hence $H = 0$ and also $q_{ij} = \text{const}$ behind the wavefront. For long enough $\tau > \tau^*$ the wave will explore all the CNN space and (11) will reduce to (1). Thus (11) also exhibits the gradient property for $\tau > \tau^*$ (Appendix 7), although its transient process is not gradient. Thus trajectories in the phase space $\Psi = \mathbb{R}_+^{NM} \times \mathbb{R}^{NM}$ of the CNN (11) tend to one of the stable steady states that defines the CIR for a given dynamic situation.

We notice that once the wavefront reaches the target image in the CNN at $\tau = \tau_{tr}$ the calculations can be stopped. Then by construction there exists at least one path starting from the agent position and ending at the target. Thus we get a first suitable approximation to the IR. Running the CNN further for $\tau > \tau_{tr}$ improves the shaping of the r_{ij} pattern in $\{\mathbb{Z}^2, \mathbb{R}_+\}$, which leads to an exponentially saturating optimization of paths.

To illustrate the dynamics of the CNN we consider an agent in a long narrow tunnel with one end blocked by an obstacle and a target in the other end (Fig. 6a). In such situation the IR becomes effectively one-dimensional. Thus we can reduce the 2D-lattice to a 1D chain oriented along the tunnel, i.e., $r_{ij}(\tau) = r_j(\tau)$. Similar to the static environment

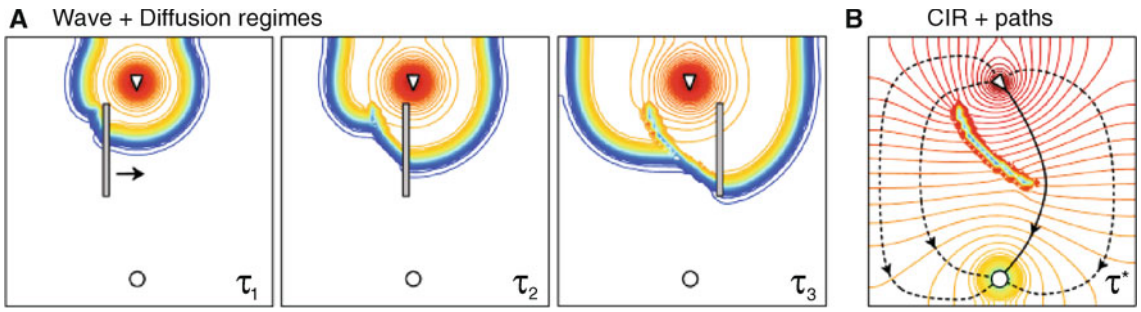

Fig. 7 Formation of the CIR of the dynamic situation sketched in Fig. 3a. **a** Three successive snapshots illustrate how the wavefront (*dense blue curves*) is affected by the virtual (simulated by the TM-RNN) motion of the obstacle. Colored curves show equipotential profiles of $r_{ij}(\tau_k)$, $k = 1, 2, 3$. **b** Final CIR after the diffusion phase. *Black solid curve* is the shortest path to the target. *Dashed paths* are safer but longer

we initialize $r_j(0) = 0$ except the cell occupied by the agent $r_0(0) = r_a$ (for simplicity we assume that the agent is one cell long). The recovery variables are set to zero for all units, $v_j(0) = 0$. Then the regime controlling function $H(r) = 1$ almost everywhere, and the effective obstacles do not exist yet, $q_j(0) = 1$ (Fig. 6b, snapshot τ_0).

Figure 6b shows several snapshots illustrating the CNN dynamics. At the beginning the *wave regime* dominates the chain. Two wavefronts running in opposite directions switch units to the upstate. Since $r_u = r_h$ this also facilitates switching of the regime controlling function $H(r)$ from 1 to 0 for these units due to the coupling force ($r_a > r_u$). Thus the FitzHugh-Nagumo dynamics is canceled and the *diffusion regime* takes over the network dynamics in the inner zone (between two wavefronts), as in Sect. 3.1. For $\tau = \tau_3$ the wavefront reaches the target and we can stop the calculations. The obtained IR offers an alternative: either go to the left, or go to the right. The latter is transient and it converts into a saddle type (unstable) path once we allow the transversal movements, i.e., obtain a quasi 2D geometry. For $\tau \to \infty$ the second option disappears.

5 Simulations: IR of different dynamical situations

Let us now test the performance of the IRNN in different simulated environments.[1]

5.1 Avoiding single moving obstacle: safety vs. speed

We begin with the dynamic situation sketched in Fig. 3a, where a single elongated obstacle crosses the arena with a constant velocity. After observing the object during the first three time steps (needed for the estimation of its initial velocity and acceleration) the TM-RNN predicts its future trajectory. This calculation is fed into the CNN where the CIR of this dynamic situation is created.

Figure 7a shows three successive snapshots of the CNN state (2D profile of r_{ij}) where for convenience we also have drawn the virtual positions of the obstacle (gray bar) calculated by the TM-RNN. The obstacle's virtual movement affects the wavefront propagating outward the target position. The lattice units, where the spatiotemporal positions of the wavefront and of the obstacle image match, correspond to effective obstacles and their dynamics is frozen (curved area behind the obstacle in Fig. 7a).

Behind the wavefront the network dynamics switches to the diffusion phase (see also Fig. 6) which finally shapes the r_{ij} pattern. This shaping does not affect the frozen cells (effective obstacles), instead virtual agents "diffuse" around them thus finding all possible ways and eventually end up at the target. Thus for a big enough τ^* the profile $r_{ij}(\tau^*)$ creates a purpose-based CIR of the dynamic situation where the potential agent motions are synchronized with the moving obstacle (Fig. 7b).

As it has been discussed above, the CIR offers multiple alternatives on how to reach the target. For example, the agent (e.g., being in a hurry) can chose the shortest path to the target (solid curve in Fig. 7b), or select a longer but safer path (dashed curves in Fig. 7b).

5.2 Nonlinear motion and gaps in effective obstacles

Let us now illustrate how relatively simple trajectories of a moving obstacle can lead to nontrivial CIRs.

We consider an obstacle moving along a parabolic trajectory (Fig. 8a), which can simulate, for example, a free fall of an object launched with initial "horizontal", $v_x(0)$, and "vertical", $v_y(0)$, velocities. For convenience the trajectory shape is fixed and we examine three cases, which differ by the obstacle velocity: (i) slow, (ii) intermediate, and (iii) fast motions.

[1] Corresponding videos can be found at http://www.mat.ucm.es/~vmakarov/IRNN.html.

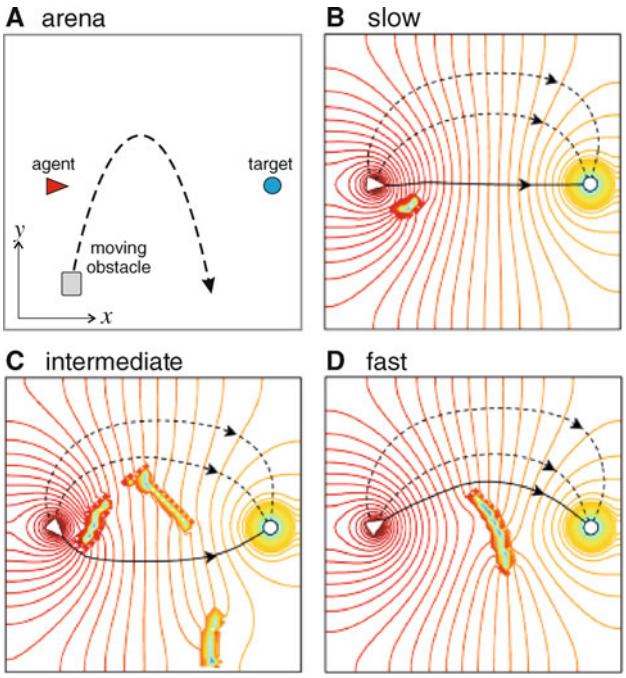

Fig. 8 Gaps in effective obstacles. **a** Dynamic situation. Obstacle (*grey rectangle*) moves along a parabolic trajectory (*dashed curve*). **b–d** CIRs of the situation significantly depend on the obstacle velocity

As we have shown above, parabolic trajectories can also be predicted by the TM-RNN. In the case of slow motion, the obstacle image coincides with the wavefront in time and space in the first (ascending) part of the trajectory only, where a small effective obstacle appears (Fig. 8b). Then the created CIR enables straight-line path to the target (solid line). We note that although this path crosses the obstacle trajectory in (x, y)-plane these intersections do not occur in the complete (x, y, τ)-spacetime. Besides the shortest the agent can select safer paths going above the obstacle trajectory (Fig. 8b, dashed curves).

Now we increase the obstacle velocity but conserving its trajectory. This significantly changes the spatiotemporal domains where the wavefront coincides with the obstacle image. We get three spatially separated domains of frozen cells in the CNN (Fig. 8c). Thus a single moving obstacle can cause several *spatially separated* effective obstacles in the CNN space. Then the diffusion finds all the gaps, and the final CIR offers to the agent a possibility to pass through the gaps. The black solid curve in Fig. 8c shows the shortest path to the target that goes below the first two effective obstacles and above the third one. Obviously, there still exist safer paths passing over the whole obstacle trajectory (Fig. 8c, dashed curves).

Finally, Fig. 8d shows the CIR for the case of a fast obstacle, whose effect on the wavefront leads to a single effective obstacle in the final (descending) part of the obstacle trajectory. Thus the shortest path to the target goes just a little bit above this effective obstacle.

5.3 Realistic environments

Realistic dynamic situations can be quite complex. For illustration we selected three particular situations.

Figure 9a (left panel) shows an example where the agent on the way to the target should go through a corridor delimited by two elongated immobile obstacles and then avoid a moving obstacle. The CIR obtained for this situation and the shortest path to the target are shown in Fig. 9a (right panel). Note that the CIR inside the corridor is essentially 1D, similar to the situation described in Fig. 6.

Figure 9b (left panel) illustrates a dynamic situation with multiple (six) moving obstacles whose simultaneous avoidance is not trivial even for living beings. The IRNN successfully solves this problem by generating a CIR with five effective obstacles (Fig. 9b, right panel). The shortest path passes between two of them.

Finally, Fig. 9c (left panel) shows a dynamic situation with a rotating (door like) obstacle. To reach the target the agent should synchronize its movement with the door. For prediction of the door position we use a slightly modified TM-RNN similar to those described in Sect. 4.1 and based on the modeling of periodic processes (Makarov et al. 2008). Depending on the rotational velocity this dynamic situation can admit (Fig. 9c, middle panel) or not (Fig. 9c, right panel) solutions. In the latter case the effective obstacle occupies all the space between the walls, thus precluding the pass. In the former case the CIR enables only passage synchronized with the door rotation, i.e., the agent, when going through, always moves between two parts composing the door. This particularly forces the agent to make a short excursion to the left in such a way that its movement synchronizes with the door rotation (dashed trajectory in Fig. 9c, middle panel).

6 Discussion

In "I of the vortex" Llinas (2001) put forward the hypothesis that "the mindness state evolved to allow predictive interactions between mobile creatures and their environment". He claimed that the capacity to predict and anticipate motions is most likely the ultimate brain function. Recently the concept of internal representation (IR) of static and dynamic situations has been strongly supported by experimental and theoretical studies. It has been shown that IR indeed offers new perspectives for the decision making and it is said to be a prerequisite for a cognitive behavior (Cruse 2003). A big challenge in the IR research is to understand how the brain makes a compact effective description of complex, time-evolving situations, in such a way that they can later be stored in (presumably static) long-term memory and then retrieved on purpose. In this paper we have proposed an IR Neural Network (IRNN) that can simulate in the phase space real

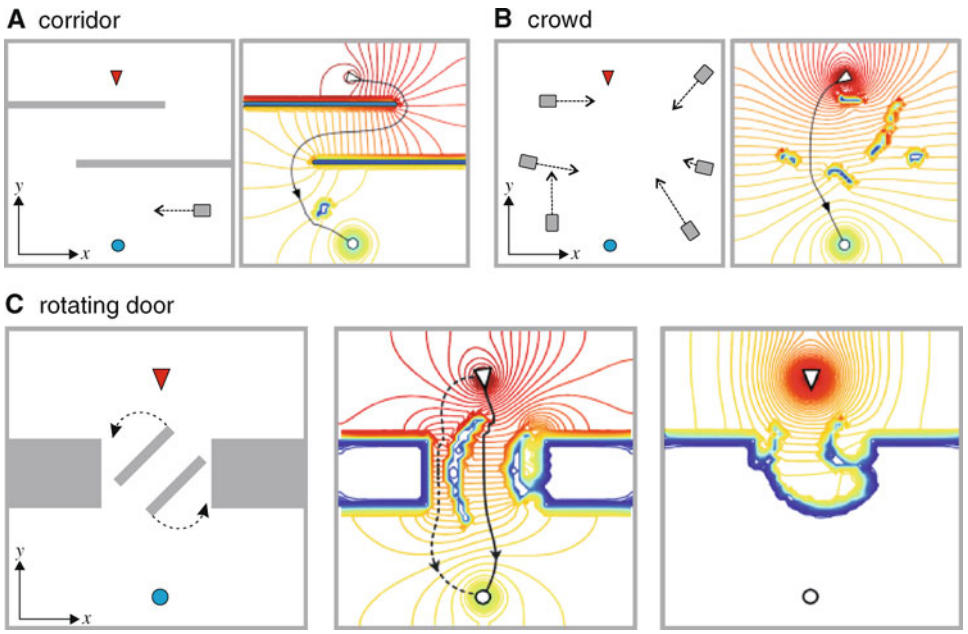

Fig. 9 Examples of CIRs of realistic dynamic situations. *Triangles* and *circles* mark the initial agent and target positions, respectively. *Grey objects* are obstacles. *Solid curves* show the shortest paths to the target. **a** Passing through a corridor and avoiding a moving obstacle. **b** Moving in a crowd environment. **c** Passing through a rotating door

world *dynamic* (i.e., time-dependent) situations and generate their time-invariant compact IRs (CIRs). We have shown that each "mental" simulation converges to a stable steady state, i.e., a single point in the network phase space describes the given dynamic situation. Besides direct on-line strategy planing for immediate motor execution, CIRs as points in a mutlidimensional space can be compared, clustered, averaged, etc. by introducing an appropriate distance measure. Libraries of stereotypic CIRs can significantly speedup and make automatic the previously learned behaviors converting them into "unconscious states". It is also noteworthy that the IRNN can work as a part of "autonomous thinking", i.e., instead of sensory information some mental situations can be supplied to the IRNN for evaluation.

The IRNN is composed of two coupled subnetworks (Fig. 1b). The Trajectory Modeling Recurrent Neural Network (TM-RNN) predicts trajectories of objects moving in the arena (Fig. 4). Noticeably, its inner structure does not depend on the features of particular movements, hence once the TM-RNN has been trained, it is ready to predict any new trajectory (belonging to a certain class). The output of the TM-RNN is fed into the Causal Neural Network (CNN) organized as a two dimensional lattice. Here we have used the simplest one-to-one mapping between the real $\mathbb{R}^2$ and the lattice $\mathbb{Z}^2$ spaces, though more complex mappings, e.g., giving preference to nearest space, are also possible. The mapping allows unfolding the steady states of the IRNN, i.e., CIRs into real space for, e.g., execution of motor actions.

Spatiotemporal synchronization of the agent movements with external elements makes up the CNN dynamics, which goes through two concurrent processes (Fig. 3). (i) The wave regime simulates parallel mental exploration of the environment. The lattice interior enclosed by the wavefront corresponds to the agent's virtual past, while the exterior belongs to its future. Then the principle of causality (i.e., the virtual future cannot influence the virtual past) allows collapsing the time-dependent structure of the dynamic situation into a static pattern, i.e., it makes the IR compact and thus biologically plausible. The propagating front ("mental present") freezes the dynamics of neurons mapping into locations of space-time coincidence of the agent and obstacles in the mental time (what we called formation of effective obstacles). (ii) The diffusion-like process shapes the states of all neurons that have not been "frozen", such that the initial excitation relaxes to a stationary 2D pattern. Thereby obtained global (steady) state of the network provides the CIR of a given dynamic situations.

CIR is an abstract construction of "what can be done", i.e., it is not reducible to a search for a best trajectory, since the solution fitness may be subjective or/and goal dependent (see, e.g., Fig. 9c). Nevertheless, one of the straightforward applications of CIRs is universal path planing, i.e., how to reach the target without collisions and taking into account the context (e.g., on the way to the target the agent should pass nearby the table) and motivation (e.g., the target has to be reached as fast as possible). We notice that the additional constraints and criteria are posed by other agent's brain areas, whereas the IRNN offers a free choice among all feasible alternative paths to the target. Using several simulated arenas, from a simple static situation (Fig. 2b) to diverse realistic environments (Figs. 7, 8, 9), we have shown that the IRNN indeed provides CIRs of complex spatiotemporal interactions between the agent and the environment. We note that a CIR

can always be created. However, actually realizable solutions (paths to the target) may not exist (Fig. 9c, right panel).

When developing the IRNN we intentionally made several simplifying assumptions on the agent and environment to disentangle influence of the main composing elements. For example, a single immobile target has been assumed; however, inclusion of several mobile targets is straightforward. Equation 2 has to be turned into time-dependent, i.e., p_{ij} will be a function of τ also predicted by the TM-RNN. Then the IRNN will allow interception of targets or selection among them. Another restriction applies to the agent, which we modeled at the very basic level. However, more sophisticated agent models, e.g., including the spatial dimensions or constraints, can also be incorporated to the IRNN, which will lead to higher realism in the modeling. Besides, the IRNN can cope with several agents cooperating or/and competing for some goals. For example, in the simplest cooperation two agents can share their actual positions and run CNNs synchronously, thus exploring much faster the environment and deciding who should do one or another task.

Finally, the generality of the IRNN approach makes it susceptible for biophysical verification. Indeed, some critical components we have introduced here already are based on biological findings (e.g., border and grid cells). Other parts, like cells "effectively frozen" under mental simulations of dynamic situations, have been postulated. Their theoretical existence is crucial for CIRs of dynamic situations. Thus the existence of border cells, firing in the presence of static obstacles, allows us to hypothesize the existence of a neuronal population that detects possible space-time coincidences of the animal and moving obstacles. The activity of these conjectured cells should simultaneously depend on the locations and velocities of the animal and obstacles. We expect that these neurons may receive an inhibitory disynaptic inputs from grid and border cells.

Acknowledgements The authors acknowledge fruitful discussions with Profs. H. Cruse and C. Avendaño. This study has been sponsored by the EU grant SPARK II (FP7-ICT-216227) and by the Spanish Ministry of Education and Science under the grant FIS2007-65173 and a Juan de la Cierva fellowship (J.A.V.).

7 Appendices

A The gradient property of (1)

Let us consider the functional

$$V = \frac{1}{2}\sum_{i,j}\left[d(r_{i+1,j} - r_{ij})^2 + (r_{i,j+1} - r_{ij})^2 + p_{ij}r_{ij}^2\right] \tag{13}$$

$V \geq 0$ and $V = 0$ for the trivial solution $r_{ij} = 0$ only. Then the dynamical system (1) can be written in the gradient form:

$$\dot{r}_{ij} = -\frac{\partial V}{\partial r_{ij}} \tag{14}$$

which implies $\mathrm{d}V/\mathrm{d}t \leq 0$. Thus stable steady states are the only attractors in the phase space $\Psi = \mathbb{R}_+^{NM}$. All trajectories of (14) are bounded for $\tau \in [0, \infty)$. Hence any initial conditions converge to one of the steady states corresponding to a local minimum of the functional V.

References

Aitkenhead MJ, McDonald AJS (2006) The state of play in machine/environment interactions. Artif Intell Rev 25:247–276

Barry C, Lever C, Hayman R, Hartley T, Burton S, O'Keefe J, Jeffery K, Burgess N (2006) The boundary vector cell model of place cell firing and spatial memory. Rev Neurosci 17(1–2):71–97

Berg BC (1993) Random walks in biology. Princeton University Press, Princeton

Berg HC, Purcell EM (1977) Physics of chemoreception. Biophys J 20:193–219

Collett TS, Zeil J (1998) Places and landmarks: an arthropod perspective. In: Healy S (ed) Spatial representation in animals. Oxford University Press, Oxford, pp 18–53

Craik K (1943) The nature of explanation. Cambridge University Press, Cambridge

Cruse H (2003) The evolution of cognition—a hypothesis. Cogn Sci 27:135–155

Cruse H, Hübner D (2008) Selforganizing memory: active learning of landmarks used for navigation. Biol Cybern 99:219–236

Hafting T, Fyhn M, Molden S, Moser MB, Moser EI (2005) Microstructure of a spatial map in the entorhinal cortex. Nature 436(7052):801–806

Holland O, Goodman R (2003) Robots with internal models—a route to machine consciousness? J Conscious Stud 10:77–109

Hesslow G (2002) Conscious thought as simulation of behaviour and perception. Trends Cogn Sci 6:242–247

Keymeulen D, Decuyper J (1994) The fluid dynamics applied to mobile robot motion: the stream field method. In: Proceedings of the IEEE international conference on robotics and automation, pp 378–385

Kuhn S, Cruse H (2005) Static mental representations in recurrent neural networks for the control of dynamic behavioural sequences. Connect Sci 17:343–360

Kühn S, Cruse H (2007) Modelling memory functions with recurrent neural networks consisting of input compensation units: II. Dynamic situations. Biol Cybern 96:471–486

Kühn S, Beyn WJ, Cruse H (2007) Modelling memory functions with recurrent neural networks consisting of input compensation units: I. Static situations. Biol Cybern 96:455–470

Llinas RR (2001) I of the vortex: from neurons to self. MIT, second printing

Louste C, Liegeois A (2000) Near optimal robust path planning for mobile robots: the viscous fluid method with friction. J Intell Robot Syst 27:99–112

Makarov VA, Song Y, Velarde MG, Hübner D, Cruse H (2008) Elements for a general memory structure: properties of recurrent neural networks used to form situation models. Biol Cybern 98:371–395

McIntyre J, Zago M, Berthoz A, Lacquaniti F (2001) Does the brain model Newton's laws? Nat Neurosci 4:693–694

Menzel R, Brandt R, Gumbert A, Komischke B, Kunze J (2000) Two spatial memories for honeybee navigation. Proc R Soc Lond B 267:961–968

Mohan V, Morasso P (2007) Towards reasoning and coordinating action in the mental space. Int J Neural Syst 17:329–341

Moser EI, Moser MB (2008) A metric for space. Hippocampus 18(12):1142–1156

Moser EI, Kropff E, Moser MB (2008) Place cells, grid cells, and the brain's spatial representation system. Ann Rev Neurosci 31:69–89

Nekorkin VI, Velarde MG (2002) Synergetic phenomenon in active lattices: patterns, waves, solitons, chaos. Springer-Verlag, Berlin

Nekorkin VI, Makarov VA (1995) Spatial chaos in a chain of coupled bistable oscillators. Phys Rev Lett 74:4819–4822

Nekorkin VI, Makarov VA, Kazantsev VB, Velarde MG (1997) Spatial disorder and pattern formation in lattices of coupled elements. Physica D 100:330–342

O'Keefe J, Dostrovsky J (1971) The hippocampus as a spatial map. Preliminary evidence from unit activity in the freely-moving rat. Brain Res 34(1):171–175

Rizzolatti G, Fogassi L, Gallese V (2001) Neurophysiological mechanisms underlying the understanding and imitation of action. Nat Rev Neurosci 2:661–670

Savelli F, Yoganarasimha D, Knierim JJ (2008) Influence of boundary removal on the spatial representations of the medial entorhinal cortex. Hippocampus 18(12):1270–1282

Schmidt GK, Azarm K (1992) Mobile robot navigation in a dynamic world using an unsteady diffusion equation strategy. In: Proceedings of the IEEE/RSJ international conference on intelligent robots and systems, pp 642–647

Sepulchre JA, MacKay RS (1997) Localized oscillations in conservative or dissipative networks of weakly coupled autonomous oscillators. Nonlinearity 10:679–713

Sharma J, Dragoi V, Tenenbaum JB, Miller EK, Sur M (2003) V1 neurons signal acquisition of an internal representation of stimulus location.. Science 300:1758–1763

Solstad T, Boccara CN, Kropff E, Moser MB, Moser EI (2008) Representation of geometric borders in the entorhinal cortex. Science 322(5909):1865–1868

Steinkuhler U, Cruse H (1998) A holistic model for an internal representation to control the movement of a manipulator with redundant degrees of freedom. Biol Cybern 79:457–466

Svensson H, Morse A, Ziemke T (2009) Representation as internal simulation: a minimalistic robotic model. In: Proceedings of the CogSci'09, 2890–2895

Taube JS, Muller RU, Ranck JB (1990a) Head-direction cells recorded from the postsubiculum in freely moving rats. I. Description and quantitative analysis. J Neurosci 10:420–435

Taube JS, Muller RU, Ranck JB (1990b) Head-direction cells recorded from the postsubiculum in freely moving rats. II. Effects of environmental manipulations. J Neurosci 10:436–447

Toussaint M (2006) A sensorimotor map: modulating lateral interactions for anticipation and planning. Neural Comput 18:1132–1155

Umiltá MA, Kohler E, Gallese V, Fogassi L, Fadiga L, Keysers C, Rizzolatti G (2001) "I know what you are doing": a neurophysiological study. Neuron 32:91–101

Vergassola M, Villermaux E, Shraiman B (2007) Infotaxis as a strategy for searching without gradients. Nature 445:406–409